predicted reflectance spectrum shows a peak at 435 nanometres with descending slopes towards both ends of the visible spectrum (Fig. 1b), which agrees well with the observed reflectance spectrum in hue (position of peak) and chroma (shape of peak). Most of the total power in the Fourier power spectrum is concentrated at spatial frequencies that will produce coherent scattering of light waves that are close to the observed blue hue. The correspondence between the peaks of the observed and predicted reflection spectra (about 75 nanometres) is striking as there are no reasons, apart from structural colour production, to expect these spatial frequencies to predominate.

In the Mie and Rayleigh scattering models, the medullary keratin scatters incoherently (which means the scatterers must be separated by distances larger than the wavelength of visible light)[8]. However, the ring-like Fourier power spectrum demonstrates that the scatterers in medullary keratin are spatially periodic on a scale smaller than visible wavelengths, so scattering is coherent. Furthermore, the air vacuoles in the medullary keratin of *C. maynana* and other structurally coloured feather barbs[3,5] are too close together to scatter visible light incoherently. Finally, the Rayleigh model predicts that the reflectance spectrum should increase continuously into the ultraviolet[1], but the distinct peak in the reflection spectrum shows this prediction to be false (Fig. 1b). Rayleigh scattering has been the traditional explanation of this phenomenon for nearly a century[4], and remains widely cited in ornithological texts and reference works[9], but our results indicate that the Rayleigh model and other incoherent scattering models are not suitable explanations.

Our analysis of the spatial variation in the refractive index of medullary keratin shows that this tissue is a highly ordered nanostructure of the appropriate size to produce the observed hue by constructive interference. The similarity in nanostructure between the medullary keratin of *C. maynana* and other structurally coloured feather barbs indicates that constructive interference probably also causes the production of the structural greens, blues, violets and ultraviolet colours in other feather barbs[1–5].

Richard O. Prum*†, Rodolfo H. Torres‡, Scott Williamson†, Jan Dyck§

**Natural History Museum, and Departments of †Ecology and Evolutionary Biology, and ‡Mathematics, University of Kansas, Lawrence, Kansas 66045, USA*
e-mail: prum@ukans.edu
§Institute of Population Biology, Universitetsparken 15, DK-2100 Copenhagen, Denmark

1. Dyck, J. *Biol. Skrift.* **18,** 1–67 (1971).
2. Dyck, J. *Z. Zellforsch.* **115,** 17–29 (1971).
3. Dyck, J. *Proc. Int. Ornithol. Congr.* **16,** 426–437 (1976).
4. Fox, D. L. *Animal Biochromes and Structural Colors* (Univ. California Press, Berkeley, 1976).
5. Durrer, H. in *Biology of the Integument* Vol. 2. *Vertebrates* (eds Bereiter-Hahn, J., Matoltsky, A. G. & Richards, K. S.) 239–247 (Springer, Berlin, 1986).
6. Finger, E. *Naturwissenschaften* **82,** 570–573 (1995).
7. Benedek, G. B. *Appl. Optics* **10,** 459–473 (1971).
8. Bohren, C. F. & Huffman, D. R. *Absorption and Scattering of Light by Small Particles* (Wiley, New York, 1983).
9. Gill, F. B. *Ornithology* (Freeman, New York, 1995).
10. Briggs, W. L. & Henson, V. E. *The DFT* (Society for Industrial and Applied Mathematics, Philadelphia, 1995).
11. *MATLAB Reference Guide* (Mathworks, Natick, MA, 1992).
12. Dyck, J. *Anser* (suppl.) **3,** 57–75 (1978).

A lower jaw from a Cretaceous parrot

All known Cretaceous bird fossils representing modern higher taxa are from the aquatic groups Anseriformes[1–3], Gaviiformes[4,5], Procellariiformes[1] and Charadriiformes[1,6]. Here I describe a toothless avian dentary symphysis (fused jawbone) from the latest Cretaceous of Wyoming, United States. This symphysis appears to represent the oldest known parrot and is, to my knowledge, the first known fossil of a 'terrestrial' modern bird group from the Cretaceous. The existence of this fossil supports the hypothesis, based on molecular divergence data[7,8], that most or all of the major modern bird groups were present in the Cretaceous.

The specimen (Fig. 1) is from UCMP locality V65238 in the Lance Formation, Lancian North American Land Mammal Age, Maastrichtian, latest Cretaceous, Niobrara County, Wyoming. The mandibular symphysis is deeply concave, with a nearly U-shaped cross-section at the posterior end of the fragment, and has a rounded anterior margin (Fig. 1). The left and right dentaries are fused completely without a suture. Small bone fibres indicate that the individual was at or close to adult size, so the characters are not juvenile states. The labial surface of the mandibular symphysis has a highly vascularized appearance, produced by numerous foramina (openings), canals and grooves for neurovascular tissue (Fig. 1c), like those present in the area in which a horny covering, or rhamphotheca, is attached to the jaw in living amniotes.

A completely fused and edentulous (toothless) mandibular symphysis is present only in turtles, oviraptorids, ornithomimids, caenagnathid theropods and neornithine birds. The pair of lingual median symphysial foramina next to the sagittal plane is found in most neornithines, including Anseriformes, Galliformes, Psittaciformes and other orders, but is absent in hesperornithiforms, oviraptorids and turtles. Caenagnathid theropods have lateral grooves, lateral occlusal grooves, lingual ridges, longitudinal vascular grooves, meckelian grooves and median tubercles[9], which

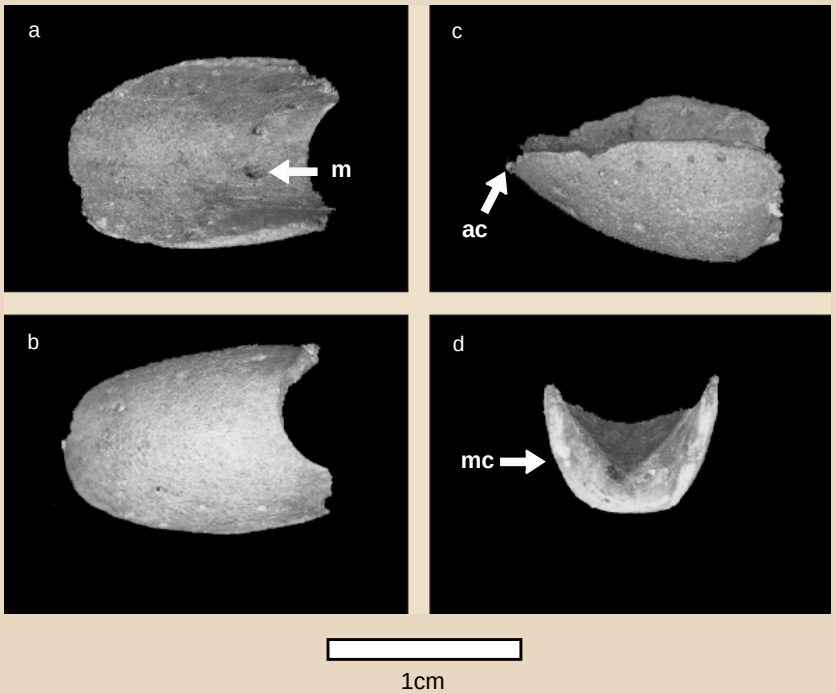

Figure 1 Mandibular symphysis of the Lance Formation parrot (University of California Museum of Paleontology, specimen UCMP 143274). a, Dorsal view. The two large median foramina (m) on the lingual surface 3.0 millimetres from the posteroventral edge of the symphysis are equidistant from the midline, with very short grooves posterior to them. b, Ventral view. c, Dorsolateral view, showing anterior accessory canal opening (ac) and large labial foramina; the right tomial crest is slightly concave, curving ventrally, and the left is worn and does not have a concave dorsal margin. d, Posterior view, showing meckelian canal (mc). Anterior is to the left in a–c.

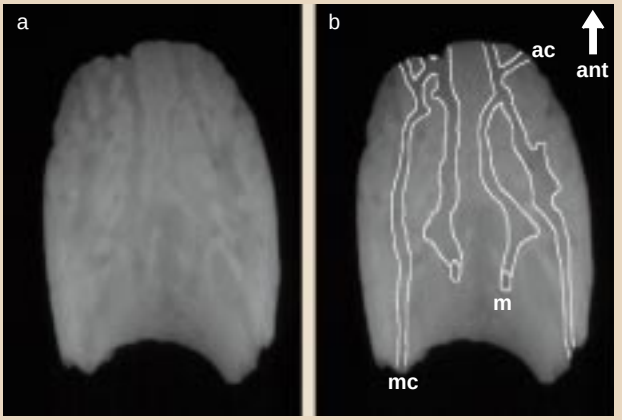

Figure 2 X-rays of the dorsoventral view of the Lance Formation parrot mandibular symphysis. a, The mandibular symphysis. b, The mandibular symphysis with the neurovascular canals outlined. The median neurovascular canals extend from the median foramina to the anterior end of the symphysis and intersect the meckelian canals. Accessory canals extend from the median canals, anterior to the intersection with the meckelian canals, anterolaterally to the tomial crest. This results in a K-shaped neurovascular canal pattern in the right side of the symphysis, with a mirror image of the pattern in the left side. Ant, anterior; other abbreviations are as in Fig. 1.

are absent in extant parrots and this specimen; the caenagnathid median symphysial foramina are located anterior to the position seen in parrots and this fossil[9]. The K-shaped neurovascular canal pattern (Fig. 2) and deeply concave symphysis seen in this specimen are apparently derived characters found only in Psittaciformes. The rounded rostral end of the symphysis, the deeply concave symphysis (compared with most Psittaciformes) and the concave tomial crest are most common in Loriidae, but also occur in some macaws and other psittacids.

The discovery of this parrot in the Lance Formation indicates that the lineage leading to the parrot crown group was present by the end of the Cretaceous. If this parrot were a lory, as suggested by its morphology, the most recent common ancestor of the psittaciform crown group would be placed in the Cretaceous[10], as supported by molecular data[11]. The occurrence of a parrot in the Cretaceous implies the presence of other closely related bird taxa in the Cretaceous, as also predicted by molecular divergence data[7,8]. These data also indicate that modern bird groups, including parrots, may have been relatively unaffected by the mass extinction at the end of the Cretaceous period.

Thomas A. Stidham
Department of Integrative Biology, Museum of Paleontology, and Museum of Vertebrate Zoology, University of California, Berkeley, Berkeley, California 94720, USA
e-mail: furcula@socrates.berkeley.edu

1. Olson, S. L. & Parris, D. *Smithson. Contr. Paleobiol.* **63,** 1–22 (1987).
2. Elzanowski, A. & Brett-Surman, M. K. *Auk* **112,** 762–767 (1996).
3. Tambussi, C. P. & Noreiga, J. I. *Ameghiniana* **32,** 57–61 (1996).
4. Chatterjee, S. *J. Vert. Paleontol. Abstr.* **9,** 16A (1989).
5. Olson, S. L. *J. Vert. Paleontol.* **12,** 122–124 (1992).
6. Brodkorb, P. in *Proc. XIIIth Int. Ornith. Congr.* (ed. Sibley, C. G.) 55–70 (American Ornithologists Union, Ithaca, NY, 1963).
7. Cooper, A. & Penny, D. *Science* **275,** 1109–1113 (1997).
8. Hedges, S. B., Parker, P. H., Sibley, C. G. & Kumar, S. *Nature* **381,** 226–229 (1996).
9. Currie, P. J., Godfrey, S. J. & Nessov, L. *Can. J. Earth Sci.* 30, 2255–2272 (1993).
10. Christidis, L., Schodde, R., Shaw, D. D. & Maynes, S. F. *Condor* **93,** 302–317 (1991).
11. Miyaki, C. Y., Matioli, S. R., Burke, T. & Wajntal, A. *Mol. Biol. Evol.* 15, 544–551 (1998).

Hydrologic cycle explains the evaporation paradox

The evaporation of water, measured using evaporation pans, has been decreasing in the past few decades over large areas with different climates. The common interpretation is that the trend is related to increasing cloudiness, and that it provides an indication of decreasing potential evaporation and a decreasing terrestrial evaporation component in the hydrologic cycle. Here we show that, although these studies are valuable, pan evaporation has not been used correctly as an indicator of climate change.

At first glance, reports of decreasing pan evaporation in European Russia, Siberia and the western and eastern United States[1], India[2] and Venezuela[3] are paradoxical. They are hard to reconcile with well-substantiated increases in global precipitation and cloudiness[4], which would normally require more surface evaporation as the only source of atmospheric water vapour, rather than less. They also run counter to predictions of increasing evaporation[5], as one of the more robust outcomes of radiative forcing, resulting from increasing atmospheric CO_2 in global circulation model calculations.

We resolve this paradox by demonstrating that, in non-humid environments, measured pan evaporation is not a good measure of potential evaporation; moreover, in many situations, decreasing pan evaporation actually provides a strong indication of increasing terrestrial evaporation.

The evaporation from a pan, E_{pa}, can be used as a good indicator of the evaporation, E, from the surrounding environment, but only when land-surface moisture is in ample supply; this normally involves multiplication by a 'pan coefficient' a of order one, depending mainly on pan type[6]. The evaporation from any large uniform land surface, with adequate moisture so available energy is the limiting factor, is usually referred to as potential evaporation, E_0. The actual evaporation from a well-watered surface is $E = E_0 = aE_{pa}$. Whenever the land-surface moisture becomes limiting and insuffiecient to sustain E_0, the actual evaporation, E, decreases below E_0 and the energy not used up by E manifests itself as an increase in sensible heat flux ΔH, such that $E = E_0 - \Delta H$. This in turn causes aE_{pa} to exceed E_0, or $aE_{pa} = E_0 + b\Delta H$, where b is another coefficient slightly larger than one, again depending mainly on pan type. Now aE_{pa} no longer provides a direct measure of E_0, so it is more appropriately called 'apparent' potential evaporation.

The main point is that E and E_{pa} exhibit complementary rather than proportional behaviour; indeed, for instance in the extreme case of a desert environment, E is zero, whereas E_{pa} is at its maximum. The idea of a complementary relationship between actual evaporation and apparent potential evaporation is not new[7], and it has stimulated advances in the estimation of terrestrial evaporation[8–10]. In the case of a pan filled with water and placed in a region with less than adequate ground wetness to sustain E_0, elimination of ΔH in the above yields $E = [(1 + b)E_0 - aE_{pa}]/b$.

Because a and b are of order one, this equation indicates how the observed[1–3] decreases in pan evaporation, E_{pa}, can be interpreted as evidence for increasing terrestrial evaporation, E, in those regions. This is consistent with data[4,11] indicating an intensifying hydrologic cycle in large regions: increasing precipitation leads to increasing surface run-off and soil wetness, which in turn generates more evaporation, and so on.

W. Brutsaert*, M. B. Parlange†
**School of Civil and Environmental Engineering, Cornell University, Ithaca, New York 14853, USA*
†Department of Geography and Environmental Engineering, Johns Hopkins University, Baltimore, Maryland 21218, USA

1. Peterson, T. C., Golubev, V. S. & Groisman, P. Y. *Nature* **377,** 687–688 (1995).
2. Chattopadhyay, N. & Hulme, M. *Agric. Forest. Meteorol.* **87,** 55–73 (1997).
3. Quintana-Gomez, R. A. Proc. 7th International Meeting on Statistical Climatology, 25-29 May 1997 (Whisler, BC, Canada, 1998).
4. Karl, T. R., Knight, R. W., Easterling, D. R. & Quayle, R. G. *Bull. Am. Meteorol. Soc.* **77,** 279–292 (1996).
5. Manabe, S. *Ambio* **26,** 47–51 (1997).
6. Brutsaert, W. *Evaporation into the Atmosphere* (Kluwer Academic, Dordrecht, 1982).
7. Bouchet, R. J. *Int. Assoc. Sci. Hydrol. Pub.* **62,** 134–142 (1963).
8. Morton, F. I. *J. Hydraul. Div. ASCE* **102,** 275–291 (1976).
9. Brutsaert, W. & Stricker, H. *Wat. Resour. Res.* **15,** 443–450 (1979).
10. Parlange, M. B. & Katul, G. G. *Wat. Resour. Res.* **28,** 127–132 (1992).
11. Lins, H. F. & Michaels, P. J. *Eos* **75,** 281, 284, 285 (1994).